

SUPPLEMENTARY DATA

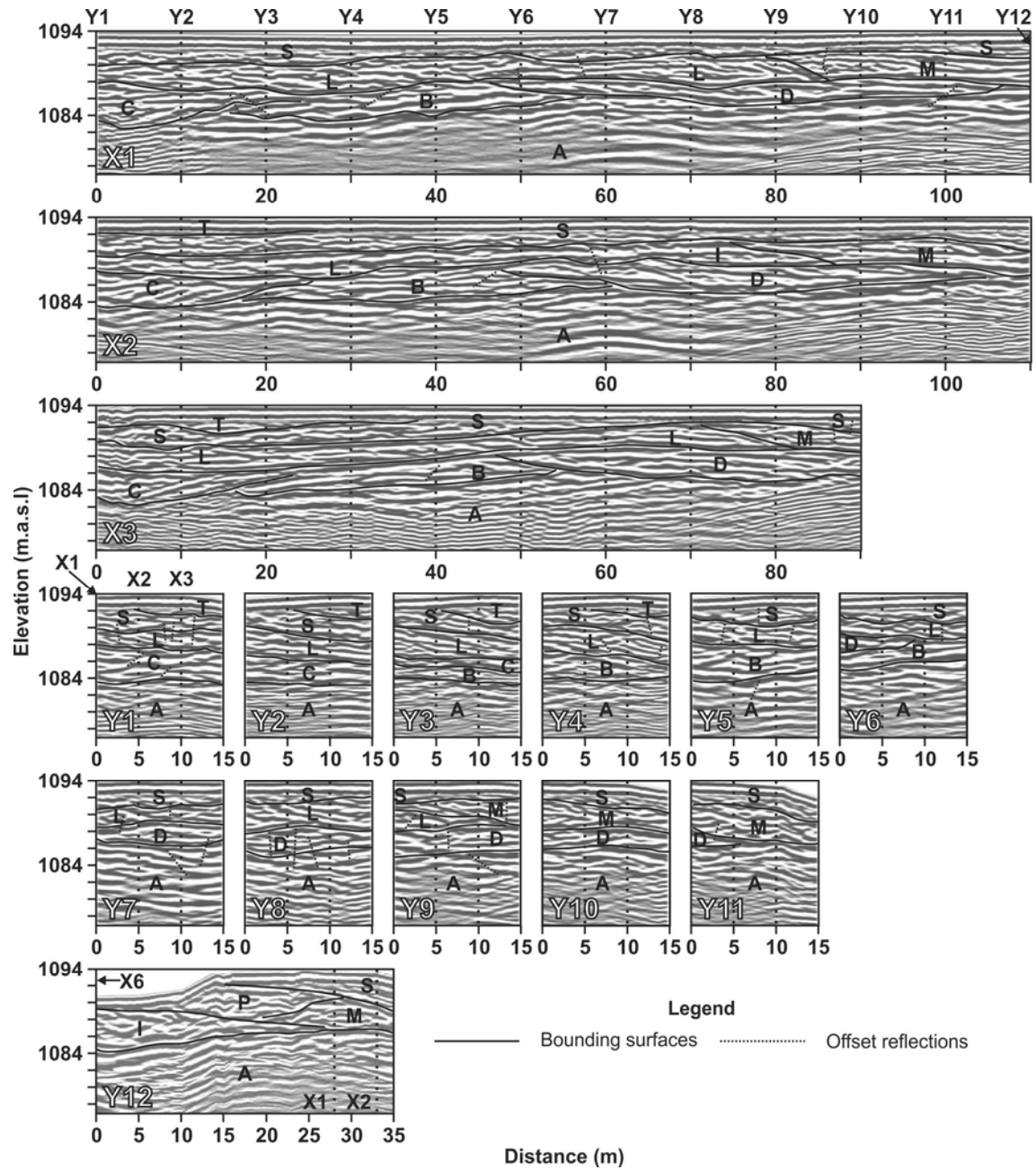


Fig. S1. Two-dimensional views of GPR profiles collected at grid 1a. The data have been processed following the protocol described in section 3.3 of the manuscript and interpreted following the method outlined in section 3.4. True relative line orientations are shown in Figure 1d. The wide dashed lines show where GPR lines intersect.

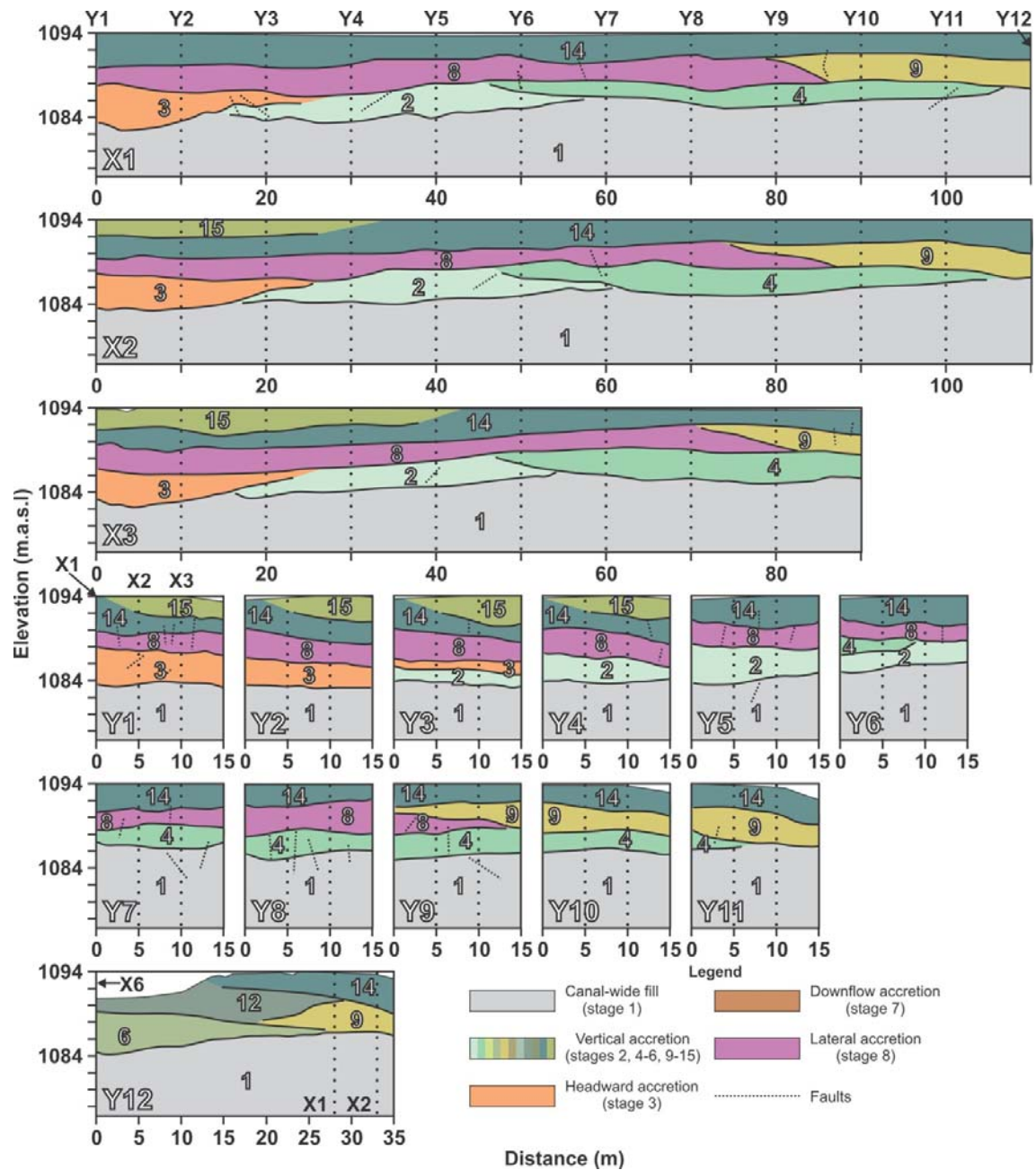


Fig. S2. Two-dimensional interpreted GPR profiles collected at grid 1a. True relative line orientations are shown in Figure 1d. Radar elements have been colour-coded based upon the broad style of deposition, using the criteria outlined in Table 1 of the manuscript. These colours correspond to those in legend (bottom right). The radar elements are numbered in order of deposition. The wide dashed lines show where GPR lines intersect.

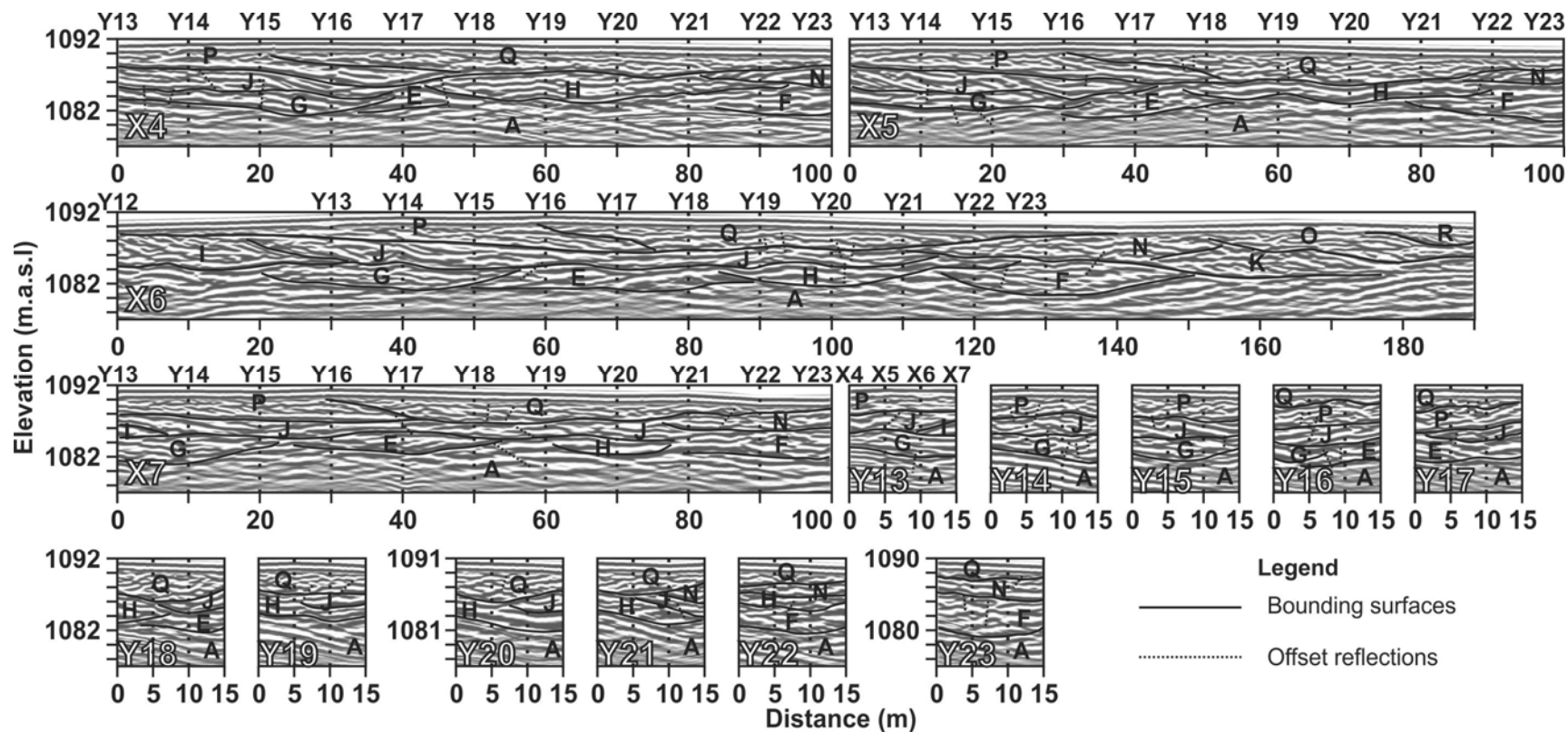


Fig. S3. Two-dimensional views of GPR profiles collected at grid 1b. The data have been processed following the protocol described in section 3.3 of the manuscript and interpreted following the method outlined in section 3.4. True relative line orientations are shown in Figure 1d. The wide dashed lines show where GPR lines intersect.

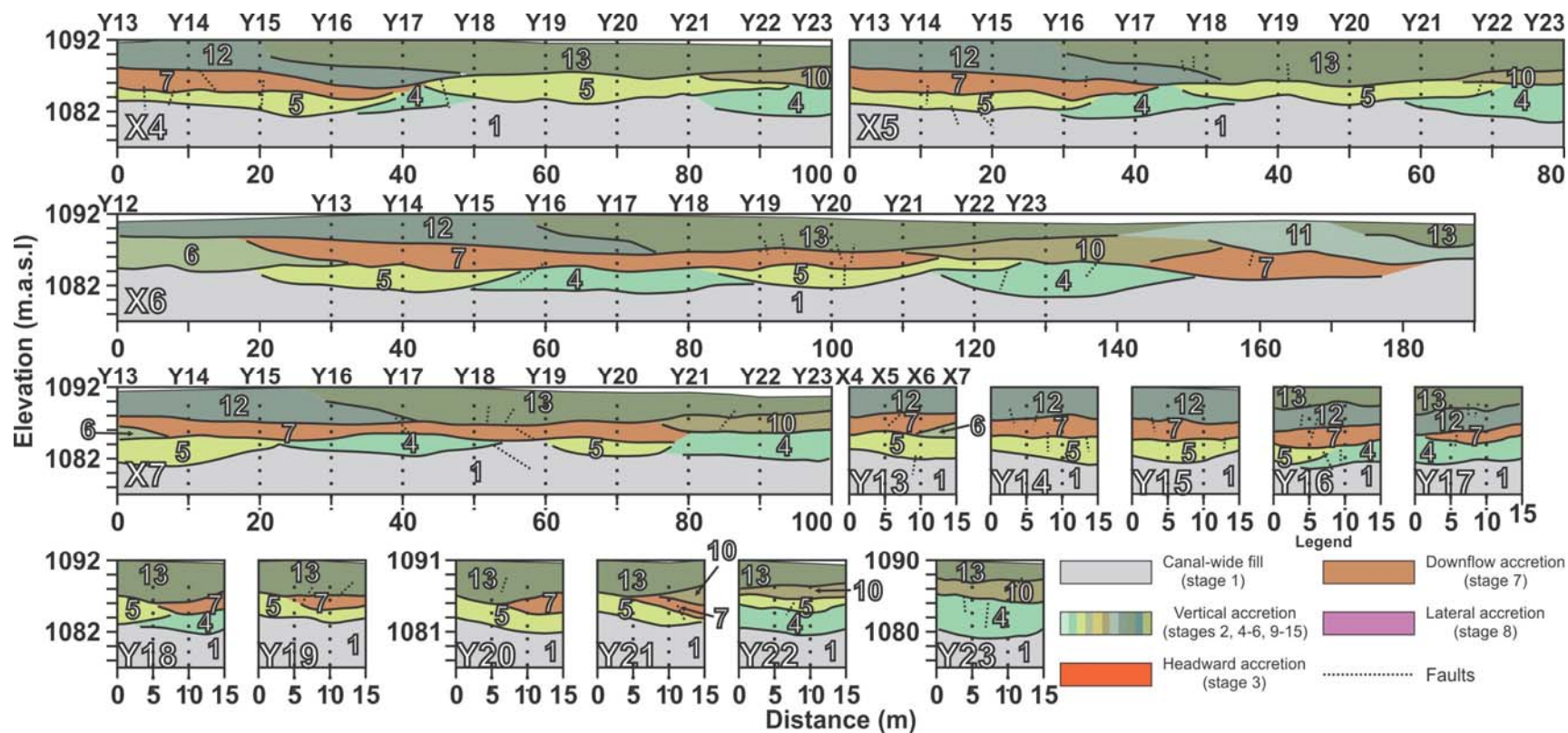


Fig. S4. Two-dimensional interpreted GPR profiles collected at grid 1b. True relative line orientations are shown in Figure 1d. Radar elements have been colour-coded based upon the broad style of deposition, using the criteria outlined in Table 1 of the manuscript. These colours correspond to those in legend (bottom right). The radar elements are numbered in order of deposition. The wide dashed lines show where GPR lines intersect.

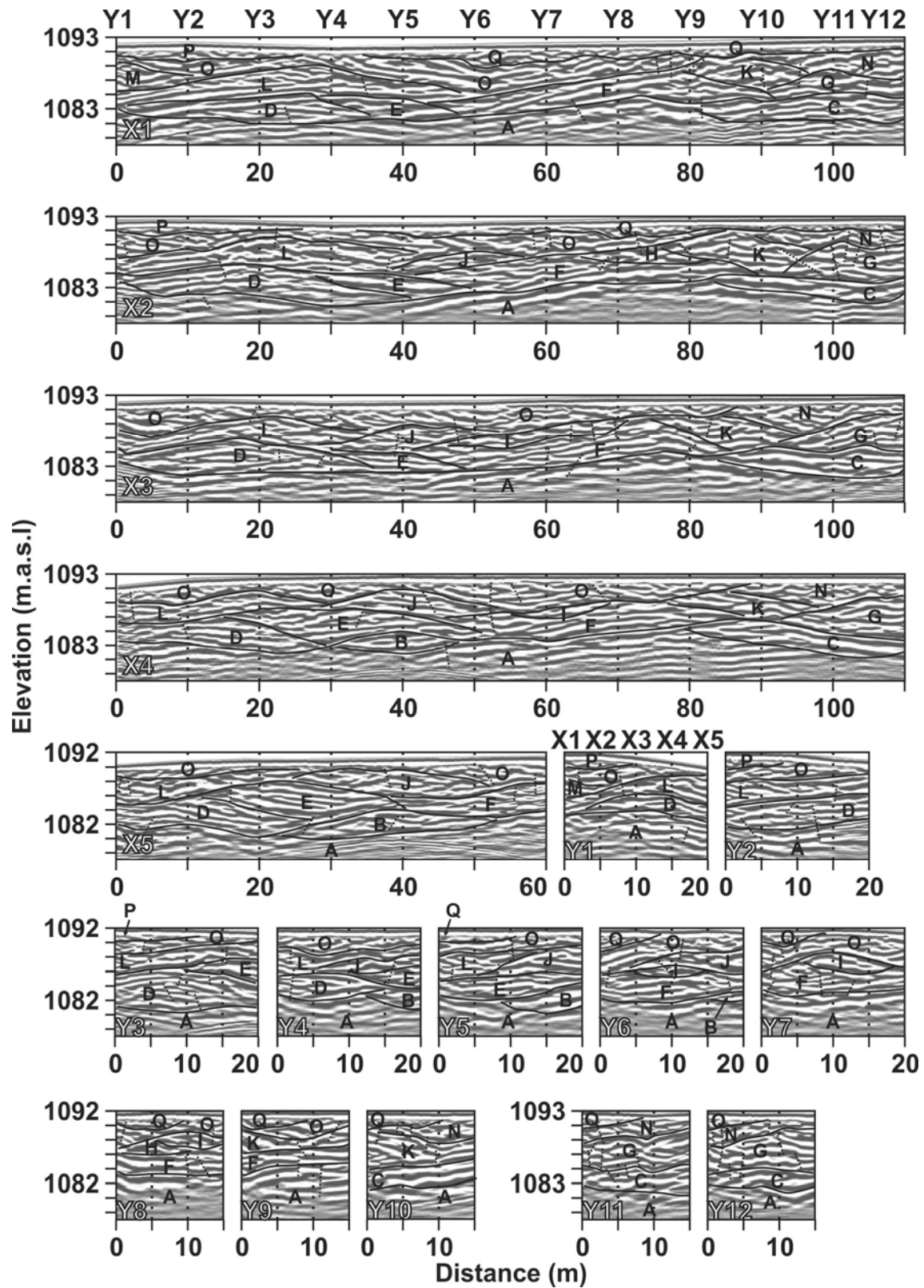


Fig. S5. Two dimensional views of GPR profiles collected at grid 2. The data have been processed following the protocol described in section 3.3 of the manuscript and interpreted following the method outlined in section 3.4. True relative line orientations are shown in Figure 1e. The wide dashed lines show where GPR lines intersect. See Fig. S1 for legend.

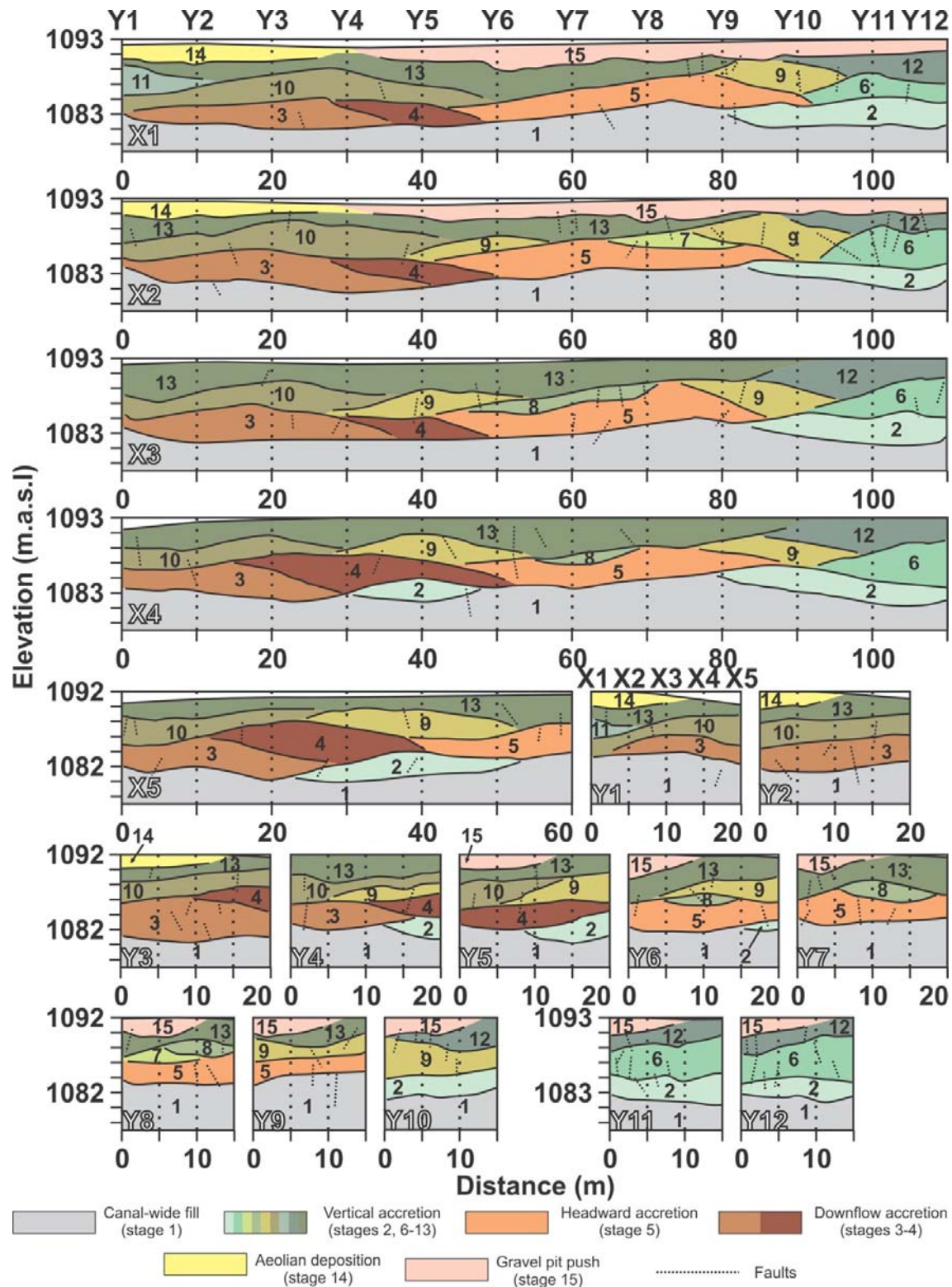


Fig. S6. Two-dimensional interpreted GPR profiles collected at grid 2. True relative line orientations are shown in Figure 1e. Radar elements have been colour-coded based upon the broad style of deposition, using the criteria outlined in Table 1 of the manuscript. These colours correspond to those in legend (bottom). The radar elements are numbered in order of deposition. The wide dashed lines show where GPR lines intersect.

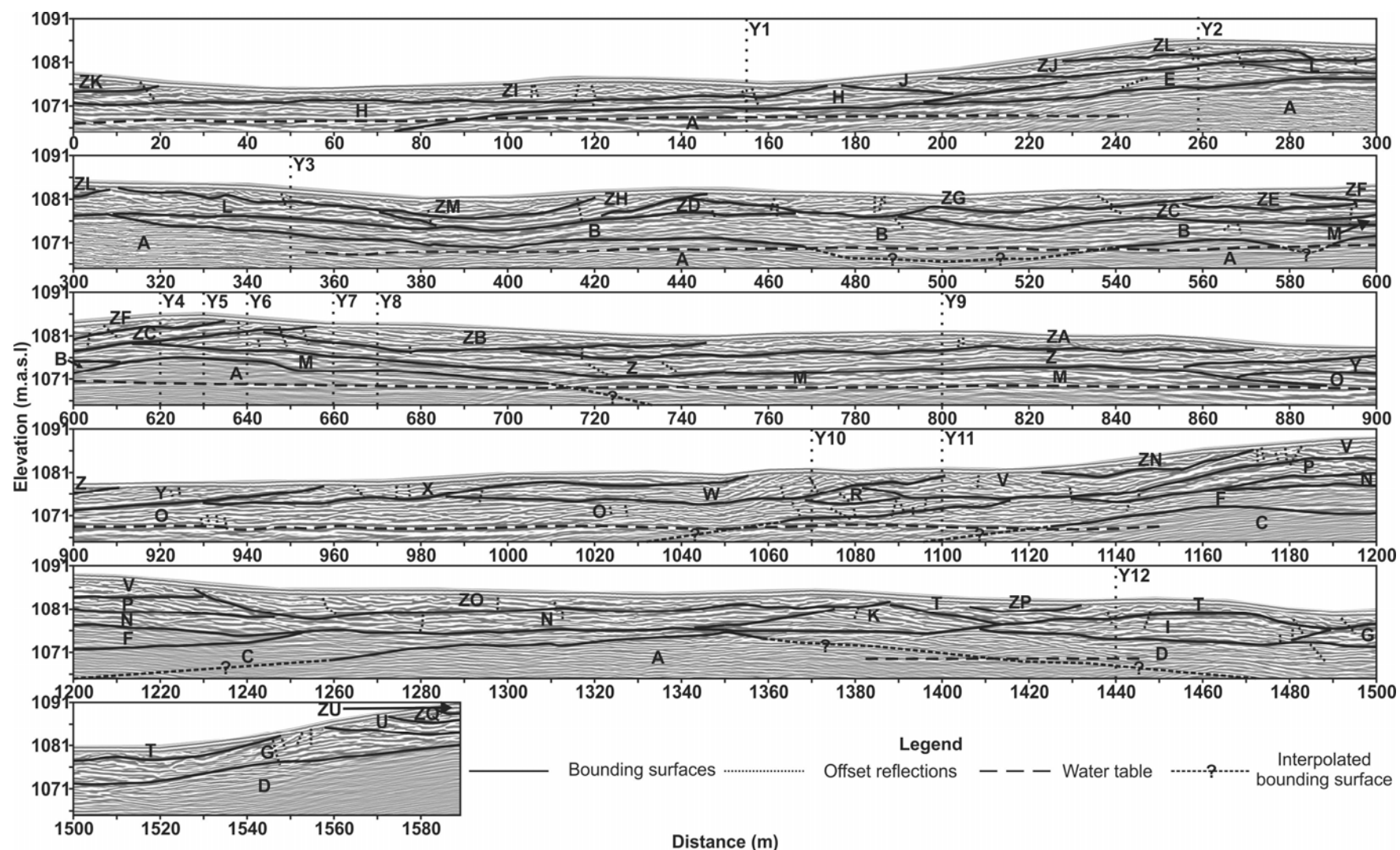


Fig. S7. Two-dimensional view of GPR line X1 of grid 3 (line is separated into sections). The data have been processed following the protocol described in section 3.3 of the manuscript and interpreted following the method outlined in section 3.4. True line orientation is shown in Figure 1f. The wide dashed lines show where GPR lines intersect.

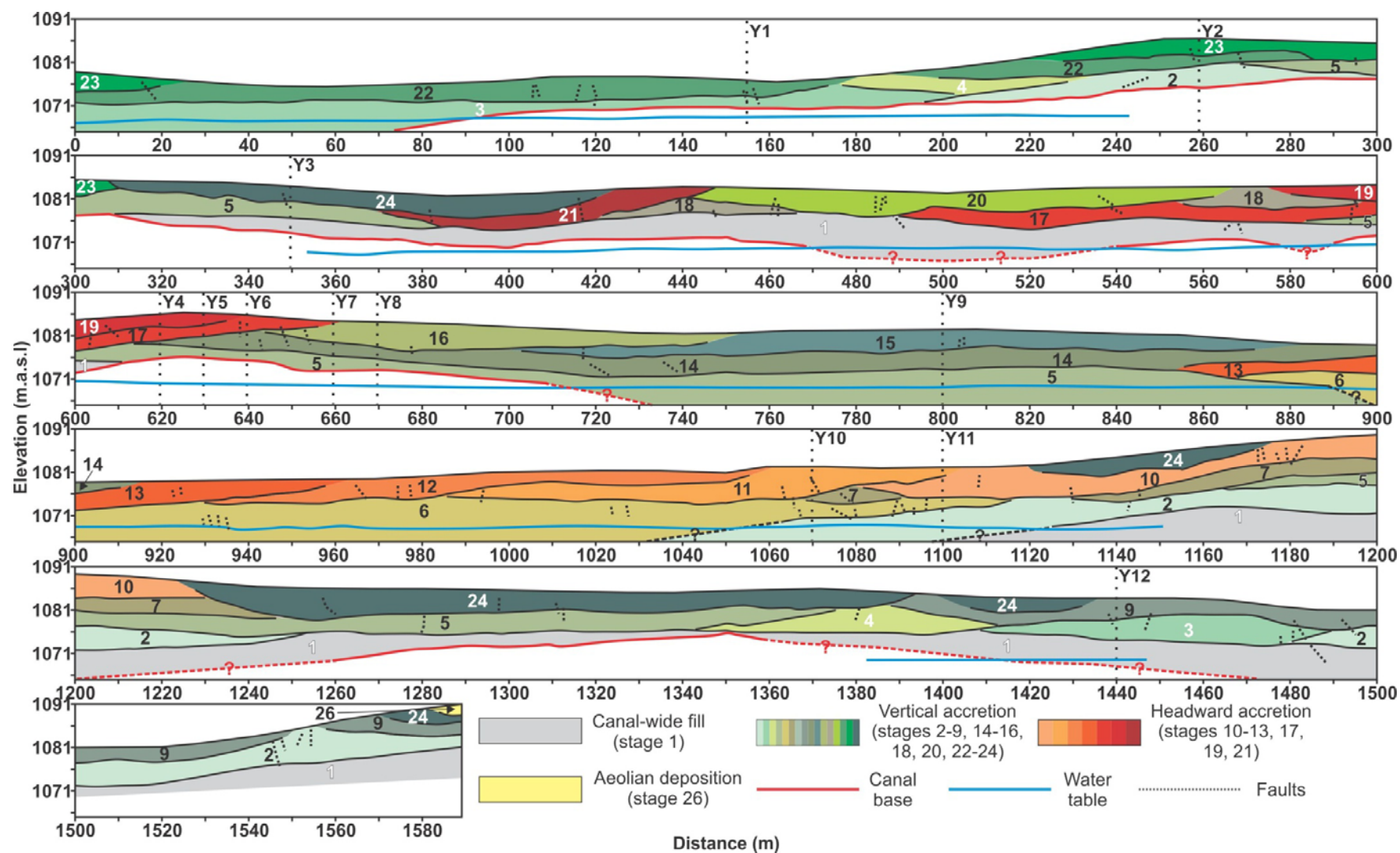


Fig. S8. Two-dimensional interpreted GPR line X1 collected at grid 3 (line is separated into sections). True relative line orientations are shown in Figure 1f. Radar elements have been colour-coded based upon the broad style of deposition, using the criteria outlined in Table 1 of the manuscript. These colours correspond to those in legend (bottom right). The radar elements are numbered in order of deposition. The wide dashed lines show where GPR lines intersect, whereas narrow dashed lines are faults.

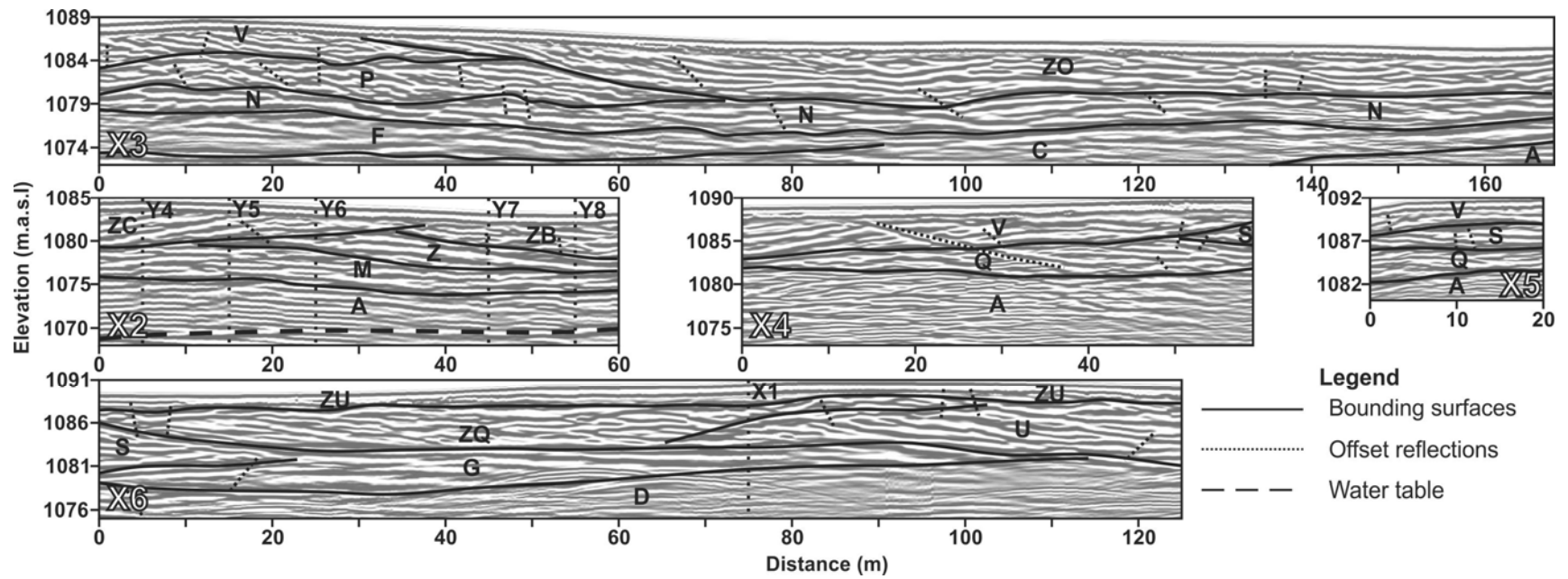


Fig. S9. Two-dimensional views of GPR lines X2-X6 collected at grid 3. The data have been processed following the protocol described in section 3.3 of the manuscript and interpreted following the method outlined in section 3.4. True relative line orientations are shown in Figure 1f. The wide dashed lines show where GPR lines intersect.

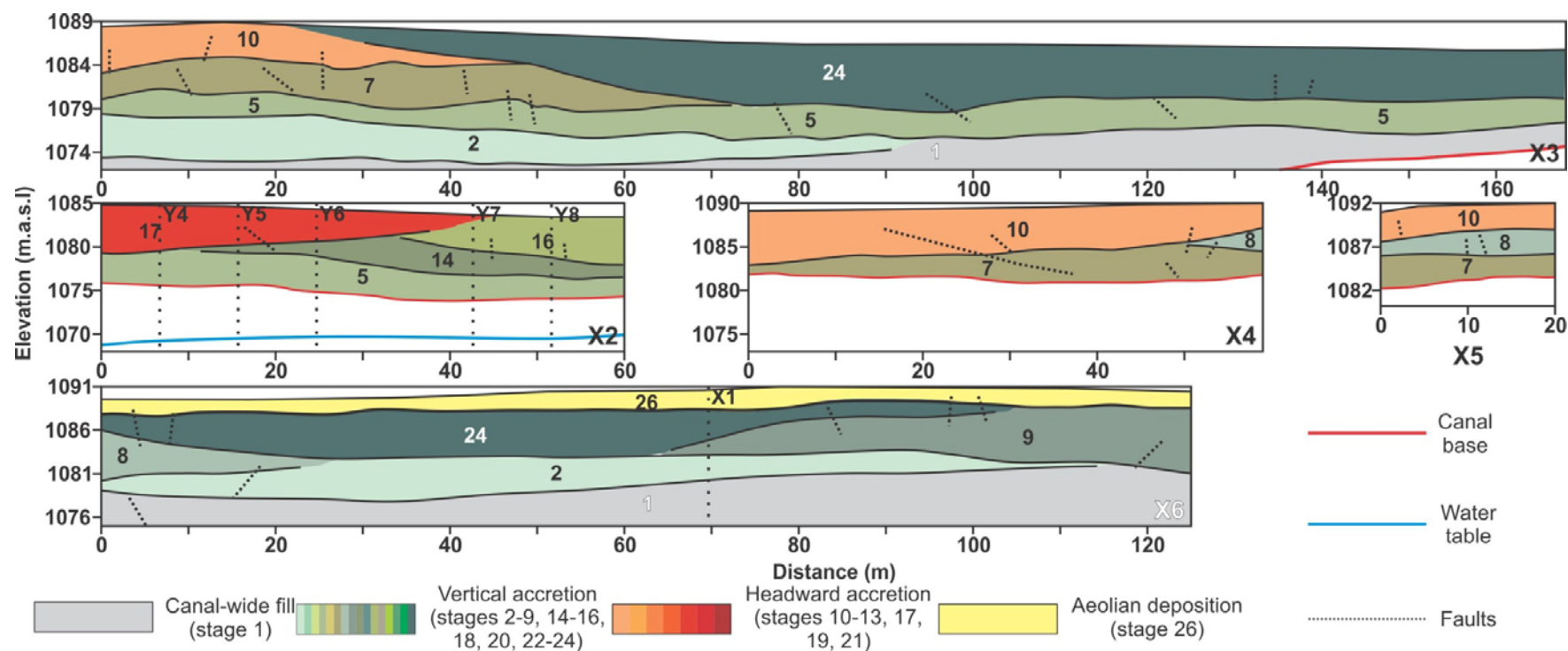
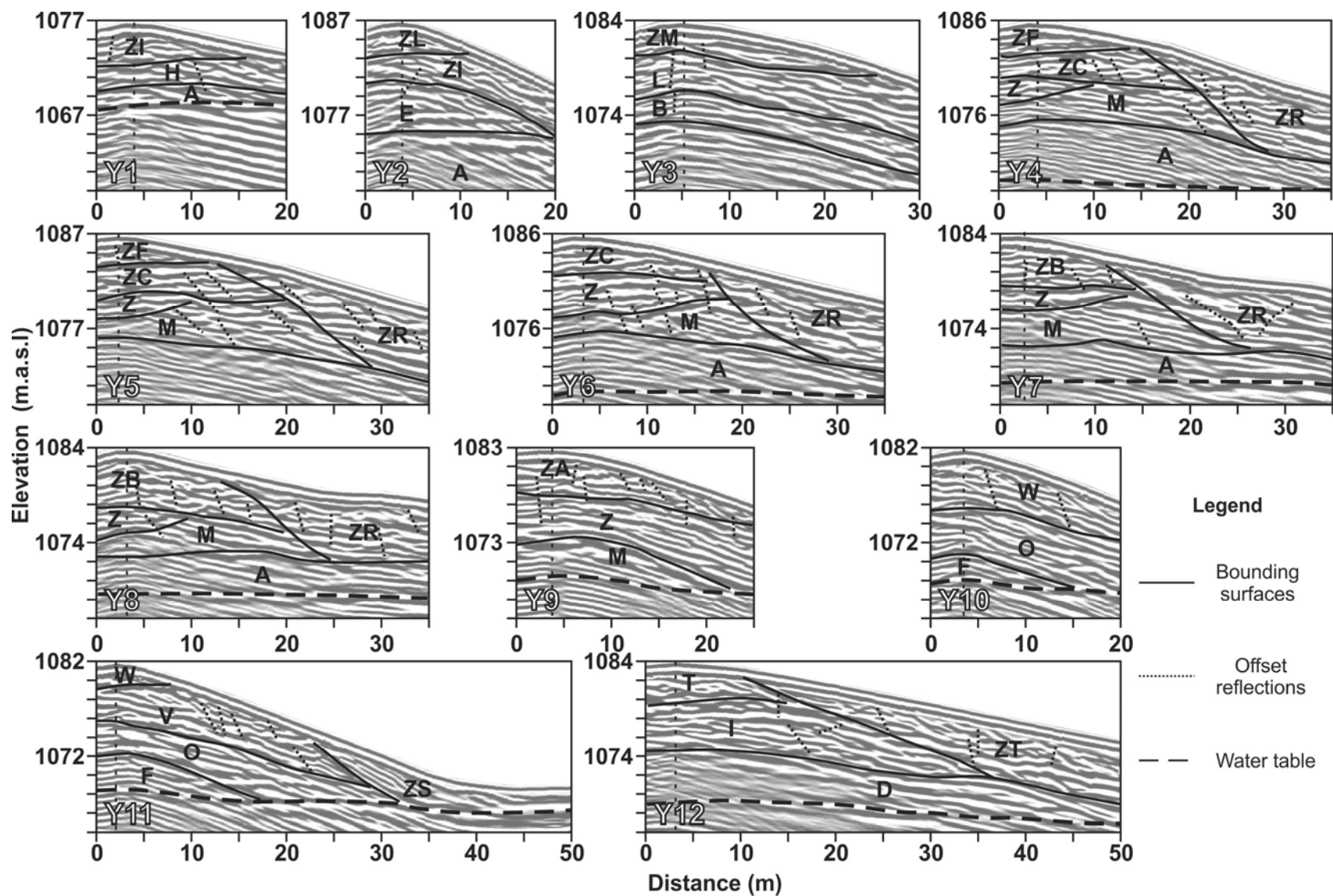


Fig. S10. Two-dimensional interpreted GPR lines X2-X6 collected at grid 3. True relative line orientations are shown in Figure 1f. Radar elements have been colour-coded based upon the broad style of deposition, using the criteria outlined in Table 1 of the manuscript. These colours correspond to those in legend (bottom). The radar elements are numbered in order of deposition. The wide dashed lines show where GPR lines intersect.



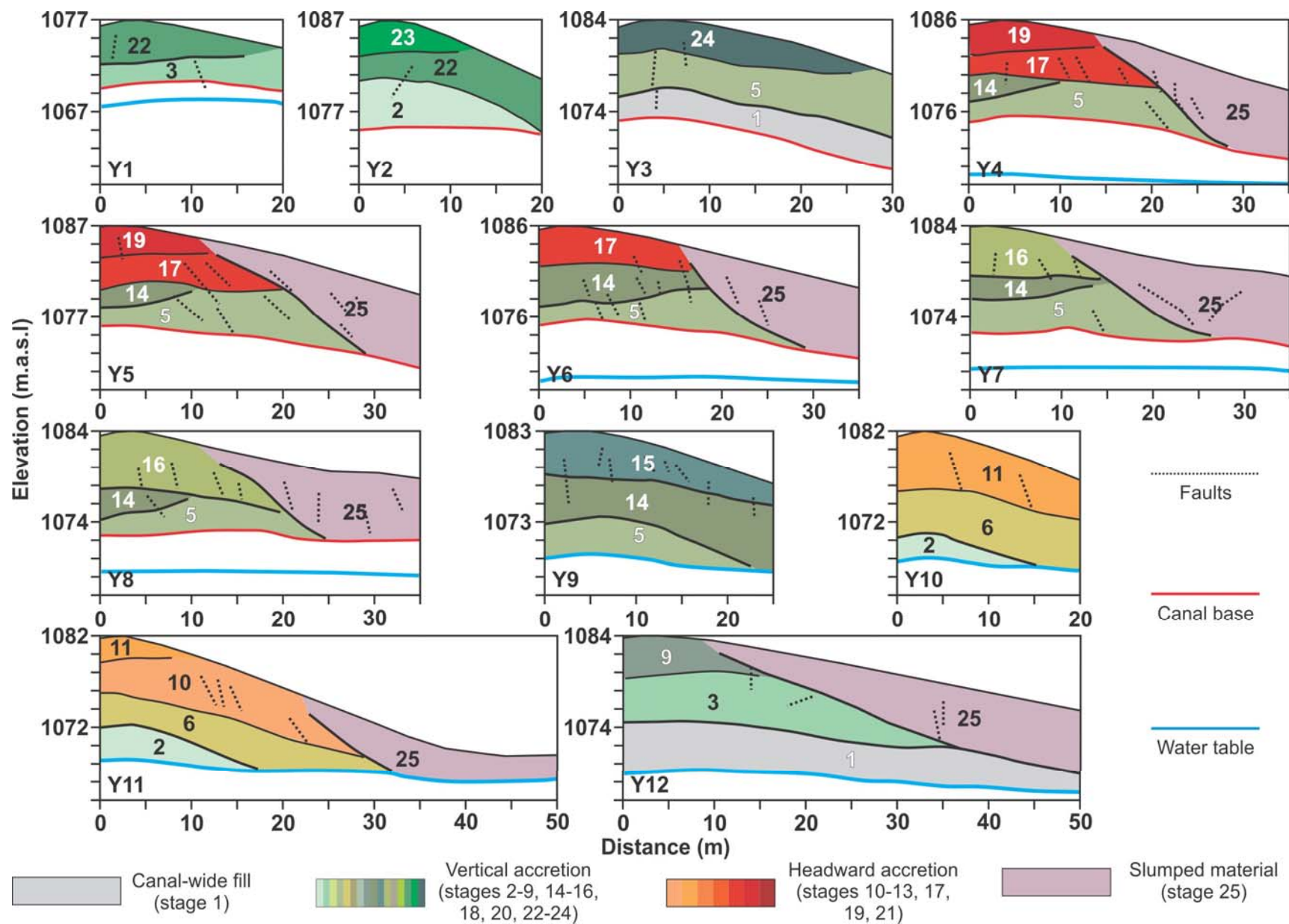


Fig. S11. [PAGE 11] Two-dimensional views of GPR lines Y1-Y12 collected at grid 3. The data have been processed following the protocol described in section 3.3 of the manuscript and interpreted following the method outlined in section 3.4. True relative line orientations are shown in Figure 1f. The wide dashed lines show where GPR lines intersect.

Fig. S12. [PAGE 12] Two-dimensional interpreted GPR lines Y1-Y12 collected at grid 3. True relative line orientations are shown in Figure 1f. Radar elements have been colour-coded based upon the broad style of deposition, using the criteria outlined in Table 1 of the manuscript. These colours correspond to those in legend (bottom right). The wide dashed lines show where GPR lines intersect.